Classification of Surface Material from Image Velocities

Katja Doerschner(1), Dan Kersten(2) and Paul Schrater(2,3)
(1) Dept. of Psychology, Bilkent University, (2) Dept. of Psychology, University of Minnesota & (3) Dept. of Computer Science & Engineering, University of Minnesota

ICVSS 2009

Bilkent, Computational & Biological Vision Group CBVG

Summary.
We propose a method for rapidly classifying surface reflectance directly from the output of spatio-temporal filters applied to an image sequence of rotating objects. Using image data from only a single frame, we compute histograms of image velocities and classify these as being generated by a specular or a diffusely reflecting object. Exploiting characteristics of material specific image velocities we show that our classification approach can predict the reflectance of novel 3D objects, as well as human perception.

Specular Flow.
The relative displacement of a specular feature or highlight due to camera or observer motion is negatively related to the magnitude of surface curvature [1, 2]. For an in-depth rotating specular ob ject (Fig. 1A) the distribution of image velocities, generated by the specular flow across the object, will have regions of relatively high and low magnitude whose specific range is directly related to the magnitude and range of surface curvatures.
This velocity variability can be exploited for reflectance classification: high image velocity variability, which can be easily identified from the image velocity histogram, appears toa be crucial to induce the spatio-temporal characteristics associated with perceived shininess [3]. Conversely, specular objects with low curvature variability will, when rotated, generate low variability image velocity distributions which are not distinct from those generated by diffusely reflecting objects (Fig. 1B).

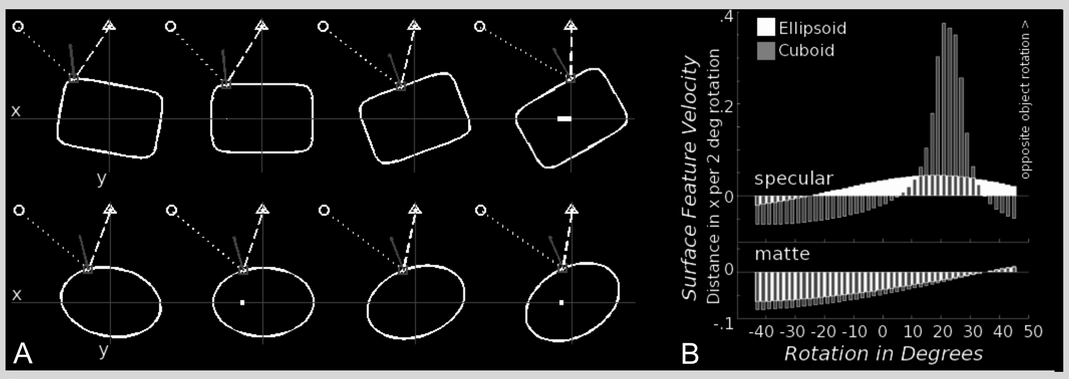

Figure 1.

Implementation.
1. Filter image sequences by spatio-temporal filters [4].

2. Estimate velocities from the filter coefficients using the max-steering method of Simoncelli [5].

3. Perform PCA on image velocities to estimate the dominant direction of motion for a given movie frame, and project image velocities onto direction vector.

4. Estimate velocity histogram densities using 3 approaches:

a) Generalized cross-entropy density estimator [6].
Use histogram estimates of conditional densities of velocity *xi* given shiny *S*, *P(xi|S)*, and matte *M*, *P(xi|M)*, from image sequences judged shiny and matte in [3]; Classify movie frame as shiny: *P(xi'|S)/P(xi'|M)>k*, where *xi'* =sample velocity, *k=.16*

b) Mixture of Gaussians with two components [7].
Classify image regions as "fast" or "slow" and project classified pixel back onto image frame; Compute velocity contrast from two estimated means: Cb=|mu1-mu2|/max (sigma1,sigma2); If Cb>1 sample is specular

c) Convolutive non-negative matrix factorization [8] with 3 components.
Estimate weights for novel sequence by maximizing likelihood of the total sample evaluated on components with respect to the weights; Use best fitting weight values to classify a sample as shiny or matte: Cw=1/2(wf1+wf3)/wf2; If Cw>1 sample is specular

5. Test Set. 36 movies (6 shapes x 6 light probes Fig. 2) of rotating specular superellipoids:

r_x=1, r_y=r_z=0.64;
n_1,n_2 = 0.3, 0.5, 0.7, 0.8, 0.9 or 1.0;
rotation in depth with respective angular speed *(0.1, 0.35, 0.61, 0.74, 0.87, 1.0* deg/frame*)*

1=[|x/r_x|^2/n_2 + |y_r_y|^2/n_2] + |z/r_z|^2/n_1

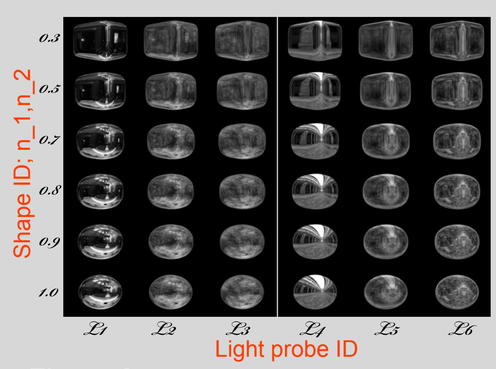

Figure 2.

Results.
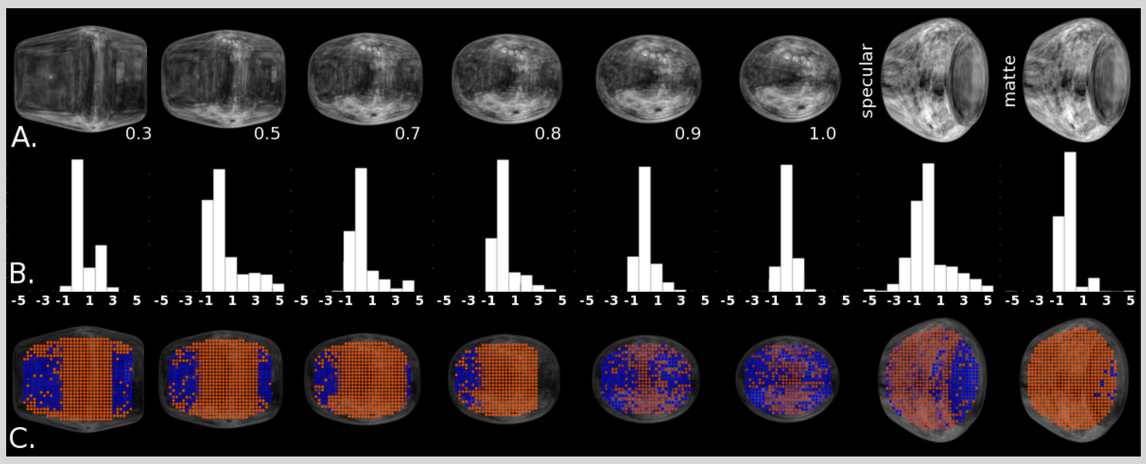

Figure 3. A. Sample frames for superellipsoids and for the specular and diffusely reflecting Utah Teapot (novel object), rendered with Radiance [9]. B. Corresponding velocity histograms. C. Corresponding pixel classification results.

Table1. Normalized Log-Likelihood Ratios. LLR > k classified as shiny with a predicted error rate of less than 5. ('T' Training data)

Table 1.

Light Probe	Superellipsoid shape coefficient n_1, n_2					
	0.3	0.5	0.7	0.8	0.9	1.0
L1	1.000^T	0.362	0.145	0.153	0.114	0^T
L2	0.961	0.362	0.184	0.215	0.139	0.031
L3	0.877	0.365	0.184	0.270	0.103	0.011
L4	0.749	0.267	0.178	0.114	0.114	0.003
L5	0.766	0.476	0.223	0.187	0.142	0.014
L6	0.805	0.368	0.159	0.187	0.148	0.003
Average	0.860	0.367	0.179	0.188	0.127	0.010

Table 2. Cb Results. When Cb>1 the histogram is classified as bimodal - a rough predictor of material shininess.

Table 2.

Light Probe	Superellipsoid shape coefficient n_1, n_2					
	0.3	0.5	0.7	0.8	0.9	1.0
Average C_b	1.658	1.4143	0.6824	0.7247	0.4778	0.1341

Figure 4. A. NNMF Results. Distribution of estimated weights across stimulus set. Ellipsoidal objects' velocity histograms (multiples of 6) tended to have high weights on component 2 (solid triangle) whereas most cube-like objects tended have high weights on components 1(circle) and/or 3(square). B. Results Cw (scaled by 1/5 for visualization) & Observer data. C. Comparison: Classification of filter coefficient (without conversion to velocities) LDA.

Figure 4.

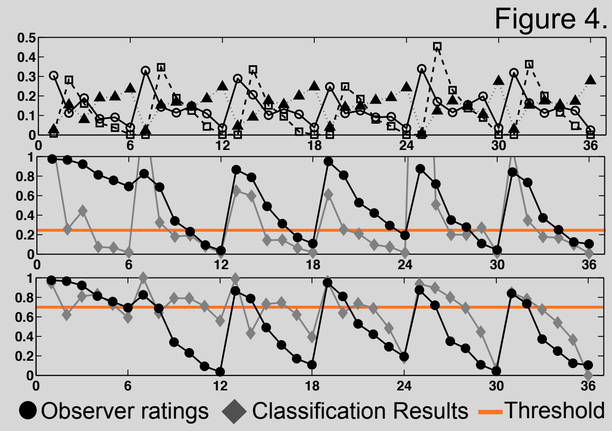

Objective classification of Novel 3D object. To verify that the velocity distribution can be sufficient for objectively classifying material we tested an object with more complex shape variation: a rotating version of the Utah "Teapot", rendered with a diffuse and with a specular reflectance (see Fig. 3A (right)). Teapots were correctly classified as specular and matte for all three methods. Histograms: LLR specular and diffusely reflecting teapot were 0.26 (classified as shiny) and 0.008 (classified as matte). Mixture of Gaussians: Cb for specular and diffusely reflecting teapot were 1.16 and 0.87 respectively. NNMF: specular teapot classified as shiny Cw=33.2, diffusely reflecting teapot classified as matte Cw= 0.7954.

Figure 5. Predicting Human Perception. In the experiment 4 observers indicated via keyboard press on a scale from 1 (matte) - 7 (mirror reflection) how shiny a given superellipsoid appeared. Normalized results are also shown in Fig. 4. Additional experimental details can be obtained from [3]. Regression of normalized LLRs (Table 1) onto normalized observer data. Training data was excluded from the regression.

Figure 5.

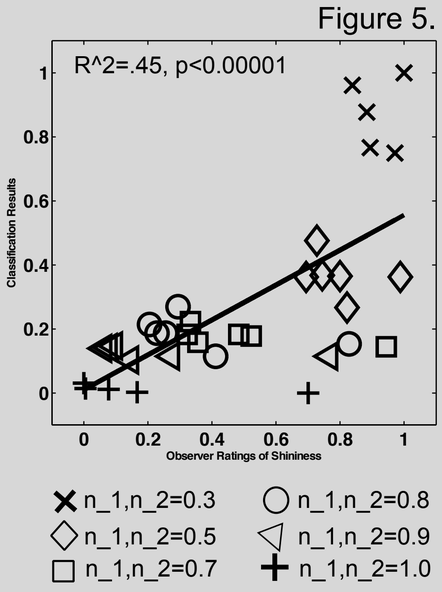

References.
1. Koenderink & van Doorn,1980; 2. Blake,1985; 3. Doerschner et al., 2007; 4. Derpanis & Gryn, 2005; 5. Simoncelli,1993; 6. Botev, 2006; 7. Nabney, 2002; 8. O'Grady & Perlmutter, 2006; 9. Ward, 1998

Contact: katja@bilkent.edu.tr